IAI Journals.ASM.org

Contributions of Environmental Signals and Conserved Residues to the Functions of Carbon Storage Regulator A of *Borrelia burgdorferi*

S. L. Rajasekhar Karna, Rajesh G. Prabhu, Ying-Han Lin, Christine L. Miller, J. Seshu

South Texas Center for Emerging Infectious Diseases, Center of Excellence in Infection Genomics and Department of Biology, The University of Texas at San Antonio, San Antonio, Texas, USA

Carbon storage regulator A of *Borrelia burgdorferi* ($CsrA_{Bb}$) contributes to vertebrate host-specific adaptation by modulating activation of the Rrp2-RpoN-RpoS pathway and is critical for infectivity. We hypothesized that the functions of $CsrA_{Bb}$ are dependent on environmental signals and on select residues. We analyzed the phenotype of $csrA_{Bb}$ deletion and site-specific mutants to determine the conserved and pathogen-specific attributes of $CsrA_{Bb}$. Levels of phosphate acetyltransferase (Pta) involved in conversion of acetyl phosphate to acetyl-coenzyme A (acetyl-CoA) and posttranscriptionally regulated by $CsrA_{Bb}$ in the $csrA_{Bb}$ mutant were reduced from or similar to those in the control strains under unfed- or fed-tick conditions, respectively. Increased levels of supplemental acetate restored vertebrate host-responsive determinants in the $csrA_{Bb}$ mutant to parental levels, indicating that both the levels of $CsrA_{Bb}$ and the acetyl phosphate and acetyl-CoA balance contribute to the activation of the Rrp2-RpoN-RpoS pathway. Site-specific replacement of 8 key residues of $CsrA_{Bb}$ (8S) with alanines resulted in increased levels of $CsrA_{Bb}$ and reduced levels of Pta and acetyl-CoA, while levels of RpoS, BosR, and other members of *rpoS* regulon were elevated. Truncation of 7 amino acids at the C terminus of $CsrA_{Bb}$ (7D) resulted in reduced $csrA_{Bb}$ transcripts and posttranscriptionally reduced levels of FliW located upstream of $CsrA_{Bb}$. Electrophoretic mobility shift assays revealed increased binding of 8S mutant protein to the CsrA binding box upstream of *pta* compared to the parental and 7D truncated protein. Two $CsrA_{Bb}$ binding sites were also identified upstream of *fliW* within the *flgK* coding sequence. These observations reveal conserved and unique functions of $CsrA_{Bb}$ that regulate adaptive gene expression in *B. burgdorferi*.

Borrelia burgdorferi, the agent of Lyme disease, is a spirochetal pathogen that is transmitted to a variety of vertebrate hosts via the bite of infected *Ixodes* ticks. *B. burgdorferi* undergoes rapid adaptation to vastly different environmental conditions present in the tick vector or the susceptible vertebrate hosts (1). A number of studies have elucidated not only the effects of one or more host-specific signals but also the contributions of relatively few regulators in modulating gene expression in *B. burgdorferi* (2–4).

Recently, a spate of studies on the regulatory networks of *B. burgdorferi* have added several layers of complexity to the molecular mechanisms that connect external signal recognition to appropriate host-specific adaptation in its disparate hosts (5–19). Expression of several key lipoproteins of *B. burgdorferi* such as outer surface protein C (OspC) and decorin binding proteins A and B (DbpA/B) that contribute to vertebrate host infection were shown to be dependent on the Rrp2-RpoN-RpoS pathway (20–23). Additional factors that contribute to *rpoS*-dependent expression of vertebrate host-specific determinants were identified, expanding the significance of this linear pathway in the pathophysiology of *B. burgdorferi* (4, 15, 16, 24, 25). Studies on activation of the Rrp2-RpoN-RpoS pathway focused on the role of a cognate histidine kinase (*hk2*) and a metabolite, acetyl phosphate, derived from phosphorylation of acetate by the enzyme acetate kinase (AckA; BB0622) (23). The conversion of acetyl phosphate to acetyl coenzyme A (acetyl-CoA) by the enzyme phosphate acetyltransferase (Pta), however, appears to play a role in the activation of the Rrp2-RpoN-RpoS pathway (23, 26, 27). Pta, in turn, is posttranscriptionally regulated by $CsrA_{Bb}$ (26). Recently, we and others have shown the importance of $CsrA_{Bb}$ in altering gene expression critical for vertebrate host-specific adaptation and virulence (28, 29). Additional reports also revealed the ability of $CsrA_{Bb}$ to directly bind regulatory elements present upstream of Pta and FlaB—the major flagellin of *B. burgdorferi* (26). However, regulation of levels of $CsrA_{Bb}$ by external signals and structure and function correlates that contribute to conserved and pathogen-specific attributes of this regulator in *B. burgdorferi* are yet to be completely delineated.

A number of studies have documented the role of CsrA and its cognate noncoding small RNAs in several Gram-negative bacteria (30–32). However, there is no evidence of cognate noncoding small RNAs of $CsrA_{Bb}$ identified in *B. burgdorferi* (26). Previous studies have shown that levels of $CsrA_{Bb}$ are upregulated when *B. burgdorferi* is propagated under conditions that mimic the midgut of ticks after a blood meal (pH 6.8/37°C) compared to those before a blood meal (pH 7.6/23°C). Moreover, levels of supplemental acetate in the borrelial growth medium impact the levels of $CsrA_{Bb}$ (27). In addition, increased levels of acetate also upregulated a solute binding protein, OppA5 (BBA34), in *B. burgdorferi* and restored levels of RpoS in an *oppA5* mutant, presumably via increased transport of acetate, with a concomitant increase in levels of acetyl phosphate (33). It is unclear if the levels of $CsrA_{Bb}$ alone or the levels of available acetate contribute to the activation of the

Received 24 April 2013 Returned for modification 16 May 2013
Accepted 29 May 2013
Published ahead of print 10 June 2013
Editor: A. J. Bäumler
Address correspondence to J. Seshu, j.seshu@utsa.edu.
Supplemental material for this article may be found at http://dx.doi.org/10.1128/IAI.00494-13.

doi:10.1128/IAI.00494-13

Rrp2-RpoN-RpoS pathway. Moreover, it also not known if alterations in the levels of extracellular acetate could remediate the phenotype observed with borrelial strain lacking *csrA*$_{Bb}$.

Sequence comparison of CsrA$_{Bb}$ with other CsrA homologs revealed conservation of several key residues in two distinct domains and the presence of 7 additional amino acids at the C terminus of CsrA$_{Bb}$ that are conspicuously absent in other homologs (34–36). Since CsrA$_{Bb}$ is unique in terms of its ability to be upregulated in response to temperature/pH and levels of acetate, elucidation of the contributions of key residues to regulation of the host-specific adaptation via Pta or FlaB would provide a greater understanding of its regulatory functions (26, 28, 29).

Since *csrA*$_{Bb}$ is the terminal open reading frame (ORF) of a large *flgK* motility operon, it is possible that the levels of CsrA$_{Bb}$ could directly or indirectly regulate multiple members of this motility operon, thereby connecting regulation of the structure/motility of *B. burgdorferi* to its virulence/colonization capabilities (28, 37). Moreover, it has been recently shown that CsrA regulates the synthesis of major flagellin (Hag) of *Bacillus subtilis* via a partner-switching mechanism whereby secretion of Hag releases FliW, which antagonizes the effect of CsrA, resulting in translational derepression of *hag* concomitant with filament assembly (31, 38–40). We, and others, have observed that increased levels of CsrA$_{Bb}$, *in trans*, result in a drastic reduction in the levels of FlaB (28, 41). While an upstream, untranslated region (UTR) of *flaB* has been shown to be a target for CsrA$_{Bb}$ binding, it is not clear if the levels of CsrA$_{Bb}$ expressed in *cis* as the terminal member of the *flgK* motility operon or the levels that are synchronized with those of other members of the *flgK* motility operon alter the levels of FlaB in *B. burgdorferi* (41).

In this study, we explored the effect of addition of acetate on the phenotype of *csrA*$_{Bb}$ deletion strain in modulating the Rrp2-RpoN-RpoS pathway via Pta. We also determined the phenotypic effects of replacement of 8 critical residues with alanines that are conserved in CsrA$_{Bb}$ and that are known to mediate interactions of CsrA with its cognate small RNAs in other bacteria. In addition, the effect of deletion of 7 C-terminal amino acids present in CsrA$_{Bb}$ was also evaluated. These analyses were done using *cis*-complemented strains such that the levels of expression/synthesis of parental and mutant CsrA$_{Bb}$ proteins were synchronized with those of other members of the *flgK* motility operon. We also determined that that there were two CsrA$_{Bb}$ binding sites upstream of *fliW* (*bb0183*) within the coding sequence of *flgK* and that the levels of FliW correlated with the levels of CsrA$_{Bb}$. These studies indicate that the functions of CsrA$_{Bb}$ are dependent on the levels of extracellular acetate and partly modulated by the regulated levels of members of the *flgK* motility operon whose terminal ORF is *csrA*$_{Bb}$.

MATERIALS AND METHODS

Bacterial strains and growth conditions. A clonal, infectious isolate of *B. burgdorferi* strain B31 (A3; see Table S1 in the supplemental material) that has all the infection-associated plasmids was used for the deletion of *csrA*$_{Bb}$ using procedures described previously (42–48). All *B. burgdorferi* cultures used for transformations were grown in 1% CO_2 at 32°C in BSK-II liquid medium (pH 7.6) supplemented with 6% normal rabbit serum (49). Spirochetes were grown to a density of 5×10^7 cells/ml in BSK-II growth medium that mimicked the tick midgut before (pH 7.6/23°C) and after (pH 6.8/37°C) a blood meal (50). Effects of supplemental acetate on *B. burgdorferi* protein levels were determined following growth in BSK-II medium that mimicked tick midgut conditions before or after the blood meal with additional 30 and 90 mM sodium acetate as described previously (27). Spirochetes were harvested at a density of 5×10^7 cells/ml. *Escherichia coli* TOP10 (Invitrogen, Carlsbad, CA) and Rosetta (DE3) pLysS (Novagen, Madison, MI) strains were used for all procedures involving cloning and overexpression of recombinant proteins, respectively. *E. coli* strains were cultured in Luria-Bertani (LB) broth supplemented with appropriate concentrations of antibiotics (27).

Expression and purification of recombinant proteins for generation of monospecific sera. Total genomic DNA obtained from *B. burgdorferi* clonal isolate MSK5 (see Table S1 in the supplemental material) was used as the template. Procedures used to generate recombinant proteins have been described previously (27). Recombinant wild-type (wt) CsrA$_{Bb}$; CsrA$_{Bb}$ with a 7-amino-acid C-terminal deletion (7S); CsrA$_{Bb}$ with 8 site-specific changes (8D); FlfB (BB0180); FlgK (BB0181); and FlgL (BB0182) were overexpressed using the vector pMAL-p2x and purified as fusion proteins with an N-terminal maltose binding protein (MBP) tag. Recombinant FliW (BB0183) with a C-terminal 6× histidine tag was generated using the vector pET23a. Recombinant proteins with MBP were purified to homogeneity using an amylose column with a Biologic Duoflow chromatography system (Bio-Rad), and His tag protein was purified using nickel-nitrilotriacetic acid (Ni-NTA) affinity column chromatography (data not shown) (27). Proteins were quantified by a bicinchoninic acid (BCA) assay (Pierce, Thermo Fisher Scientific, Rockford, IL) and stored at −80°C until further use. The purified recombinant proteins were emulsified in equal volumes of Titermax (Sigma, St. Louis MO) and used to immunize 6-to-8-week-old female BALB/c mice (46). Booster immunizations were given at days 14 and 21. Immunoblot analysis was carried out to determine the specificity of the antibodies against the recombinant proteins and total borrelial lysates with the serum obtained on day 28 postimmunization (data not shown) (46). All animal procedures were done in accordance with the approved animal use protocol from the Institutional Animal Care and Use Committee of The University of Texas at San Antonio.

Generation of *csrA*$_{Bb}$ mutant in *B. burgdorferi* B31-A3 strain. The plasmid pES10 was previously used to generate a *csrA*$_{Bb}$ deletion strain in *B. burgdorferi* B31 lacking lp25 (ML23) (29). The same construct was used to electrotransform B31-A3 and mutant colonies counterselected with 50 μg/ml of streptomycin (42, 43). Deletion of *csrA*$_{Bb}$ was confirmed by PCR (Fig. 1B) and by Southern hybridization (data not shown). One clone designated A3-ES10 was used for further studies and has the same plasmid profile as the parental strain except for the loss of cp9 (data not shown).

Generation of *cis*-complemented strains carrying the *csrA*$_{Bb}$ wild type or truncated *csrA*$_{Bb}$ (7D) or *csrA*$_{Bb}$ alleles with site-specific changes (8S). A plasmid designated pSR49 containing an approximately 2.2-kb fragment corresponding to a chromosomal region of *csrA*$_{Bb}$ was generated with an engineered SalI restriction site to facilitate cloning of the gentamicin resistance marker under the control of constitutive borrelial promoter P$_{flgB}$ downstream of *csrA*$_{Bb}$ and upstream of BB0185. The primer set of P1 and P2 was used to generate an approximately 1.1-kb fragment, including the *csrA*$_{Bb}$ and its upstream region, and the primer set of P3 and P4 was used to generate a similarly sized fragment corresponding to the downstream region of *csrA*$_{Bb}$. Overlapping PCR was done with appropriate primer pairs, and an approximately 2.2-kb amplicon was cloned into pCR2.1 vector. This resulted in the generation of a SalI site between the upstream *csrA*$_{Bb}$ and the downstream amplicons. The SalI site in the plasmid pSR49 was used to insert two tandem copies of a P$_{flgB}$-GentR marker (where "GentR" represents gentamicin resistance) to generate pSR50, which was used to restore a functional copy of wild-type *csrA*$_{Bb}$ in A3 ES-10. Electrotransformation of A3-ES10 was carried out as described above. The rationale for using two tandem copies of P$_{flgB}$-GentR was our ability to readily isolate mutants with site-specific changes in CsrA$_{Bb}$ as described below and to have an identically constructed *cis*-complemented strain carrying a parental copy of *csrA*$_{Bb}$ in A3-ES10 replacing the streptomycin resistance cassette. Primer pairs were designed to replace each of the 8 conserved residues of CsrA$_{Bb}$ in conjunction with pSR49 containing

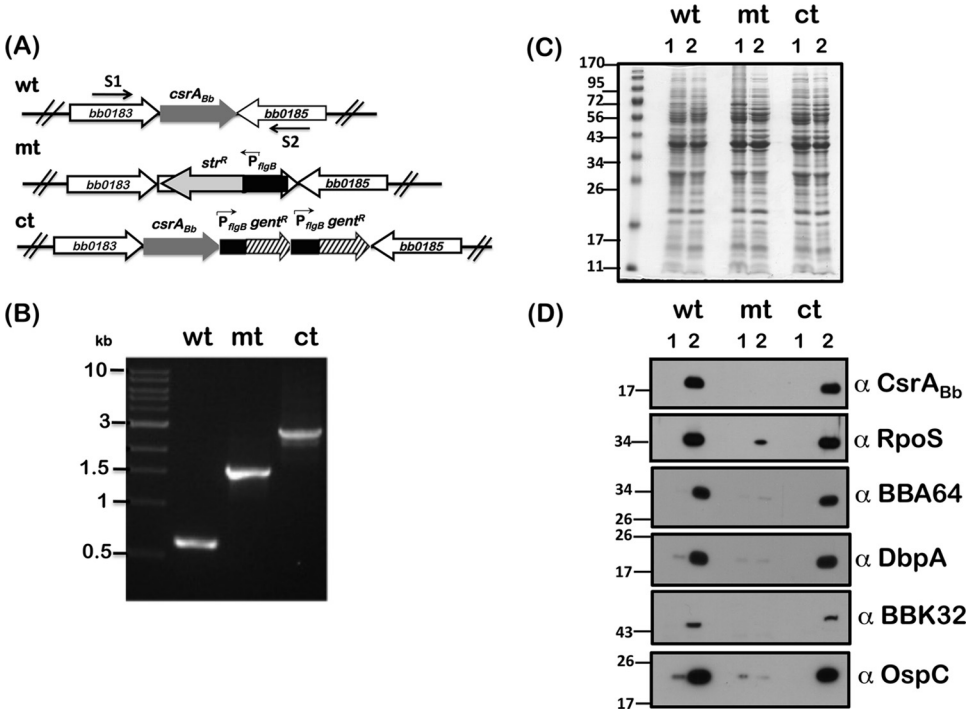

FIG 1 Generation of *csrA*$_{Bb}$ deletion and *cis*-complemented strains in *B. burgdorferi* strain B31-A3. (A) Schematic representation of the region of *csrA*$_{Bb}$ in the chromosome of *B. burgdorferi* strain B31-A3 (wt). A *csrA*$_{Bb}$ deletion strain was generated by replacing *csrA*$_{Bb}$ with P$_{flgB}$-streptomycin (*str*^{R}; mt), and a *cis*-complemented strain was generated by restoring a functional copy of *csrA*$_{Bb}$ in *cis* with downstream P$_{flgB}$-gentamicin (*gent*^{R}, ct). Arrows indicate orientations of primers S1 and S2 used to screen the mutant and *cis*-complemented strains. (B) Ethidium bromide-stained 1% agarose gel depicting amplicons generated using primers S1 and S2 specific to upstream and downstream regions of *csrA*$_{Bb}$. Total genomic DNAs from wild-type (wt), *csrA*$_{Bb}$ mutant (mt), and *cis*-complemented (ct) strains were used as the template. Molecular mass markers in kilobases are indicated to the left. (C) Total protein profiles of wild-type (wt), *csrA*$_{Bb}$ mutant (mt), and *cis*-complemented (ct) strains propagated under conditions mimicking the tick vector before (lanes 1; pH 7.6, 23°C) or after (lanes 2; pH 6.8, 37°C) a blood meal. Equivalent amounts of proteins were separated on an SDS–12.5% polyacrylamide gel and stained with Coomassie blue. Molecular mass markers in kilodaltons are indicated to the left. (D) Immunoblot analysis of the borrelial strains shown in panel C with antisera against CsrA$_{Bb}$, RpoS, BBA64, DbpA, BBK32, and OspC. Blots represent one of three independent experiments.

the parental CsrA$_{Bb}$ as the template using a QuikChange site-directed mutagenesis kit (Stratagene). Once the first conserved residue was replaced with alanine, the resulting plasmid was used as the template to replace the next conserved residue using appropriate primer sets (see Table S2 in the supplemental material). A plasmid designated pRG50 was generated where all 8 critical residues of CsrA$_{Bb}$ were replaced with alanines (35, 36) and was used to clone P$_{flgB}$-GentR in the SalI restriction enzyme site present downstream of the mutant *csrA*$_{Bb}$ and *bb0185* to generate a plasmid designated pRG59 (see Fig. 5; see also Table S1 in the supplemental material). A mutant B31-A3 clone designated 8S carrying site-specific changes in 8 critical residues was isolated. Primers P1 and P5 were used to generate a truncated *csrA*$_{Bb}$ without the DNA coding for the 7 C-terminal residues in the *csrA*$_{Bb}$ gene, and the plasmid generated was electrotransformed to generate the C-terminal truncated mutant. Counterselection was done using 50 μg/ml of gentamicin in BSK-II agar overlays, the isolated clones were characterized further by PCR, and sequencing of the PCR products was done to verify the changes incorporated in the mutant *csrA*$_{Bb}$ alleles.

Sodium dodecyl sulfate-polyacrylamide gel electrophoresis (SDS-PAGE) and immunoblot analysis. *B. burgdorferi* whole-cell lysates were prepared and separated on SDS–12.5% PAGE as described previously (27). The separated proteins were either visualized by Coomassie brilliant blue staining or transferred onto a polyvinylidene difluoride (PVDF) membrane (Amersham Hybond-P; GE Healthcare, Buckinghamshire, United Kingdom) and subjected to immunoblot analysis as described previously (29). The membranes were probed with monoclonal antibodies or monospecific serum against a variety of borrelial proteins. The blots were developed following incubation with appropriate dilutions of horseradish peroxidase (HRP)-conjugated anti-mouse, anti-rabbit, or anti-rat secondary antibodies using ECL Western blotting reagents (GE Healthcare). Densitometric analysis was done on select blots using ImageJ software, and statistical analysis was done using blots from three independent experiments and Student's upaired *t* test in Prism v 4.0 (see Fig. S1, S2, and S3 in the supplemental material).

RNA extraction and quantitative real-time PCR analysis. Transcriptional analysis of key genes relevant to this study was done using quantitative real-time PCR analysis. Total RNA was extracted as previously described from *B. burgdorferi* cultures propagated under conditions (pH 6.8/37°C) that resulted in increased levels of CsrA$_{Bb}$ to a density of 2×10^7 to 3×10^7 spirochetes per ml (29). The total RNA was treated twice at 37°C for 45 min with DNase I to remove any contaminating DNA and quantified spectrophotometrically. The purity of the RNA sample was assessed using real-time PCR with *recA* primers (recAFq and recARq) to rule out presence of contaminating DNA. RNA samples were reverse transcribed to cDNA using TaqMan reverse transcription (RT) reagents (Applied Biosystems, Foster City, CA). Real-time PCRs were set up with SYBR green PCR master mix with various oligonucleotide primers (see Table S2 in the supplemental material) at a final concentration of 100 nM, and quantitative real-time PCR was done using an ABI Prism 7300 system (Applied Biosystems) as described previously (29). The threshold cycle (C_T) values for each of the genes were averaged following normalization, the levels of induction were determined with the $\Delta\Delta C_T$ method, and the quantity of each transcript was determined by the $2^{-\Delta\Delta CT}$ method, where the C_T value is the cycle number of the detection threshold, as described

TABLE 1 Infectivity analysis of $csrA_{Bb}$ mutant in C3H/HeN mice at 21 days postinfection

Strain and dose (no. of spirochetes/mouse)	No. of cultures positive/no. tested							No. of mice infected/no. tested
	Skin	Spleen	Joint	Lymph node	Heart	Bladder	All sites	
wt (B31-A3)								
10^3	3/3	2/3	3/3	3/3	3/3	3/3	17/18	3/3
10^5	3/3	3/3	3/3	3/3	3/3	3/3	18/18	3/3
mt (A3-ES10)								
10^3	0/3	0/3	0/3	0/3	0/3	0/3	0/18	0/3
10^5	0/3	0/3	0/3	0/3	0/3	0/3	0/18	0/3
ct (A3-SR50)								
10^3	3/3	1/3	3/3	3/3	3/3	3/3	16/18	3/3
10^5	3/3	3/3	3/3	3/3	3/3	3/3	18/18	3/3

previously. The normalized C_T values obtained for the ct, 7S, and 8D strains were subjected to an unpaired Student's *t* test implemented in PRISM. Statistical significance was accepted when the *P* values were less than 0.05.

EMSAs. RNA probes specific to 5′ untranslated regions (UTRs) of *pta* (*bb0589*) and *fliW* (*bb0182*) were synthesized and biotinylated using a BrightStar psoralen-biotin labeling kit (Ambion) per the manufacturer's suggested protocol. Electrophoretic mobility shift assays (EMSAs) were done as described previously with minor modifications (26). rCsrA-wt, rCsrA-7D, rCsrA-8S, and MBP alone (control) at the indicated picomolar concentrations were incubated with biotinylated RNA (20-fmol) probes, 40 ng yeast RNA, and 10 U of RNase inhibitor (Applied Biosystems) in a 10-μl reaction buffer (10 mM Tris-HCl [pH 7.5]; 100 mM KCl; 10 mM $MgCl_2$; 10 mM dithiothreitol; 10% glycerol). A single *pta* RNA probe with a $CsrA_{Bb}$ binding site was used to determine the binding efficiency of wild-type and mutant $CsrA_{Bb}$ proteins, while three different *fliW* RNA probes containing both binding sites (wild type) or with one site mutated (BS1 or BS2 mutated) or both sites mutated (BS1 and BS2 mutated) were used. RNA-protein complexes were allowed to occur for 30 min at 37°C, and complex formation was analyzed using 4% to 20% native polyacrylamide gels. Migration of biotinylated RNA probes was detected using a chemiluminescent nucleic acid detection module per the protocol of the manufacturer (Thermo Scientific, Rockford, IL).

Determination of levels of acetyl-CoA in $csrA_{Bb}$ mutant strains. Borrelial strains (ct, 7D, and 8S) were propagated at either 23°C/pH 7.6 or 37°C/pH 6.8 to a density of 5×10^7/ml or 1×10^8/ml, respectively, and cell lysates (total of 1×10^9 spirochetes) were prepared using perchloric acid as described previously (26). Following incubation with 3 M ice-cold perchloric acid for 30 min on ice, supernatants were collected by centrifugation and neutralized with saturated potassium bicarbonate. Levels of acetyl-CoA in the lysates were measured using a Picoprobe acetyl-CoA assay kit (Biovision Research Products, Mountain View, CA) per the manufacturer's suggested protocol.

Infectivity studies. Groups ($n = 3$) of 6-week-old female C3H/HeN mice were inoculated intradermally with either 10^3 or 10^5 spirochetes per mouse with the following borrelial strains: the wild-type strain (B31-A3), a mutant strain (A3-ES10), and a complemented strain (A3-ES10/$csrA_{Bb}^+$). At 21 days after inoculation, the spleen, left tibiotarsal joint, left inguinal lymph node, heart, bladder, and a piece of abdominal skin were collected and cultured in BSK-II growth medium to facilitate isolation of spirochetes as previously described (44, 45). The cultures were scored for growth of *B. burgdorferi* after 2 to 3 weeks using dark field microscopy. All animal procedures were performed in accordance with the animal use protocol approved by Institutional Animal Care and Use Committee (IACUC) at the University of Texas at San Antonio.

RESULTS

Restoration of parental phenotype upon *cis*-complementation of deletion mutant with wild-type $csrA_{Bb}$. We reconstructed a mutant using the B31-A3 strain that has all the critical plasmids required for infectivity by replacing $csrA_{Bb}$ with a streptomycin resistance marker under the control of a constitutive borrelial promoter, P_{flgB} (42, 51). The $csrA_{Bb}$ deletion mutant (designated A3-ES10 [mt]) was identified by PCR using primers (S1 and S2) specific to the upstream and downstream regions of $csrA_{Bb}$, resulting in an amplicon of 1,582 bp in the A3-ES10 strain (Fig. 1A and B, mt). This increase in size was due to the replacement of $csrA_{Bb}$ with P_{flgB}-StrR (where "StrR" represents streptomycin resistance) compared to a 628-bp amplicon observed with the B31-A3 parental strain (Fig. 1A and B, wt). We also restored a functional wild-type copy of $csrA_{Bb}$ in *cis* using plasmid pSR50, which had two tandem copies of a gentamicin resistance marker under the control of P_{flgB}, enabling us to readily obtain a *cis*-complemented clone designated A3-SR50 (Fig. 1A, ct). A 2.35-kb amplicon was obtained using primer set S1 and S2 that indicated the presence of $csrA_{Bb}$ and two tandem copies of P_{flgB}-GentR when total genomic DNA was used from the A3-SR50 (ct) strain (Fig. 1B, ct). We regenerated a $csrA_{Bb}$-deficient strain in an infectious isolate (B31-A3) and a *cis*-complemented strain to serve as controls to analyze the phenotype of mutant alleles of $csrA_{Bb}$.

Immunoblot analysis of these strains with anti-CsrA serum showed reactivity to only the wt and ct strains propagated at pH 6.8/37°C, while no reactivity was observed with the mt strain (Fig. 1D, α-CsrA). The sera generated against $CsrA_{Bb}$ in mice recognize an approximately 18-kDa protein in the control strains, reflecting the dimeric form of the protein. Consistent with previous reports, immunoblot analysis of $csrA_{Bb}$ mutant showed reduced levels of RpoS and products of other *rpoS*-regulated genes such as BBA64, DbpA, BBK32, and OspC compared to the wild-type and complemented strains (Fig. 1D, lanes 2, wt, mt, and ct). The *in vitro* phenotype was also consistent in that the levels of $CsrA_{Bb}$, RpoS, and *rpoS*-regulated determinants were higher under conditions mimicking those of the midgut of fed ticks (Fig. 1D, lanes 2) compared to those of unfed ticks (Fig. 1D, lane 1). Moreover, consistent with previous reports, the $csrA_{Bb}$ strain was incapable of colonization of C3H/HeN mice following intradermal needle inoculation whereas the control strains were capable of infection with both inocula (Table 1). Since our present study relied on comparing strains complemented with either wild-type or mutant $csrA_{Bb}$ alleles, it was critical to derive these strains with similar genetic modifications even though we and others have previously reported *in vitro* and *in vivo* effects of *B. burgdorferi* lacking $csrA_{Bb}$ (26, 28, 29, 41). Those earlier studies relied on *trans*-complemen-

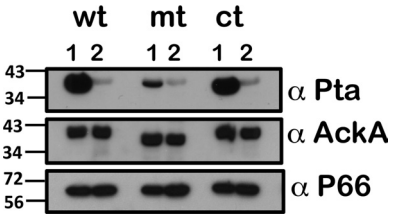

FIG 2 Immunoblot analysis of proteins involved in acetate metabolism in *B. burgdorferi*. Lysates of the wt, mt, and ct strains shown in Fig. 1C were analyzed using antisera against Pta, AckA, or P66. Horseradish peroxidase (HRPO)-conjugated secondary antibodies were used, and blots were developed with an enhanced chemiluminescence (ECL) system. Blots represent one of three independent experiments. Molecular masses in kilodaltons are indicated to the left.

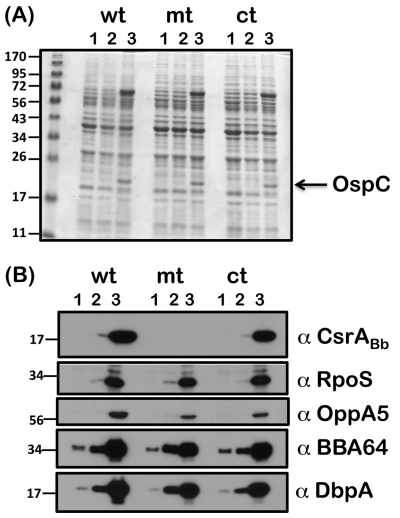

FIG 3 Immunoblot analysis of RpoS and *rpoS*-regulated proteins in the $csrA_{Bb}$ mutant grown with supplemental acetate. The wt, mt, and ct strains were propagated in BSK-II medium with 0 (lanes 1), 30 (lanes 2), or 90 (lanes 3) mM supplemental acetate at 37°C. Equivalent levels of proteins were loaded on SDS–12.5% PAGE and were either stained with Coomassie blue (A) or electrotransferred to PVDF membranes (B). The blots were probed with antisera against $CsrA_{Bb}$, RpoS, OppA5, BBA64, and DbpA and developed using an ECL system. Blots represent one of three independent experiments. Molecular masses in kilodaltons are indicated to the left.

tation of $csrA_{Bb}$ on a shuttle vector to restore $csrA_{Bb}$ function in the mutant (29, 41). We rationalized that, since $csrA_{Bb}$ is the terminal ORF of a large motility operon, mutational analysis using *cis*-complemented strains would allow analysis of phenotypic effects of $csrA_{Bb}$ under the control of its native promoter and in conjunction with other *cis- and trans*-acting factors located upstream that could impact the transcriptional and translational levels of $csrA_{Bb}$. Consistent with this expectation, our *cis*-complemented strain carrying parental $csrA_{Bb}$ had *in vitro* and *in vivo* phenotypes comparable to those of the wild-type strain while carrying gentamicin resistance markers.

Pta levels are not elevated in the $csrA_{Bb}$ mutant. Previous studies have indicated that the levels of Pta (BB0589) determine the balance between acetyl phosphate and acetyl-CoA and that $CsrA_{Bb}$ directly represses *pta* expression by binding to an element in the upstream region of BB0588 (26). We expected the levels of Pta to be elevated under all growth conditions used for the $csrA_{Bb}$ mutant if $CsrA_{Bb}$ was the only repressing regulatory molecule acting on *pta* transcripts and that the accumulation of *pta* transcripts would be independent of other signals. The levels of Pta, as expected, were increased in wt and ct strains grown at pH 7.6/23°C in a manner concomitant with lower levels of $CsrA_{Bb}$. Moreover, there were decreased levels of Pta when these strains were grown at pH 6.8/37°C that coincided with increased levels of $CsrA_{Bb}$ (Fig. 2, wt, ct; lanes 2, α-Pta). Unexpectedly, the levels of Pta were drastically lower in the $csrA_{Bb}$ mutant under unfed-tick-specific conditions compared to the control strains (Fig. 2, wt, mt, and ct; lanes 1, α-Pta). Pta levels under the fed-tick conditions were similar in all 3 strains (Fig. 2, wt, mt, and ct; lanes 2, α-Pta). Immunoblot analysis also revealed that the levels of acetate kinase (AckA [BB0622]), which converts acetate to acetyl phosphate, were similar in all three strains and under both growth conditions (Fig. 2, α-AckA). Similarly, the levels of P66, a surface-exposed porin, were similar in all three strains and served as a loading control. Taken together, these observations indicated that while increased levels of $CsrA_{Bb}$ repressed *pta* posttranscriptionally in the control strains, the levels of Pta were not drastically elevated in the $csrA_{Bb}$ deletion mutant under all conditions. This suggested that other mechanisms of regulation of *pta* are also operative in *B. burgdorferi* that could lead to increased levels of *pta* transcripts subjected to posttranscriptional regulation by $CsrA_{Bb}$. It should be pointed out that the levels of Pta in the $csrA_{Bb}$ mutant under fed-tick conditions were similar to the control strain levels (Fig. 2, lanes 2, α-Pta). The latter observation also suggested that the levels of acetyl phosphate accumulation in $csrA_{Bb}$ were insufficient for activation of the Rrp2-RpoN-RpoS pathway, as with the control strains (Fig. 1D).

Increased acetate restores levels of RpoS in $csrA_{Bb}$ mutant. We hypothesized that reduced levels of acetate accumulation within the $csrA_{Bb}$ mutant could contribute to lower acetyl phosphate levels, leading to damping of the activation of the Rrp2-RpoN-RpoS pathway. In addition, reduced acetate levels within $csrA_{Bb}$ mutant could result in reduced *pta* transcription and translation that would be independent of the levels of $CsrA_{Bb}$. As shown in Fig. 3, propagating the wt, mt, and ct strains with increasing concentrations of supplemental acetate resulted in comparable increases in the levels of RpoS, BBA34, BBA64, and DbpA in all three strains under conditions mimicking those in fed ticks (Fig. 3B, wt, mt, and ct; lanes 2). Increased levels of OspC were readily detectable on a Coomassie blue-stained gel in all three strains propagated with 90 mM supplemental acetate (Fig. 3A, wt, mt, and ct; lanes 3). It is also possible that the increased levels of OppA5 in the mutant supplemented with 90 mM acetate could have contributed to increased accumulation of acetate/acetyl phosphate overcoming the effects of *pta* in the absence of its repressor (Fig. 3B, wt, mt, and ct; lanes 3, α-OppA5).

Effect of increased acetate levels on Pta. Since intracellular levels of acetate could alter the levels of acetyl phosphate—the substrate for Pta—we determined if increased extracellular acetate would alter the levels of Pta in the $csrA_{Bb}$ mutant and contribute to the activation of the *rpoS* regulon as indicated in Fig. 3. Immunoblot analysis revealed that increased levels of acetate at pH 7.6/23°C did not alter the levels of Pta in the mutant (Fig. 4A, mt; α-Pta). However, in the control strains, the levels of Pta were detectably lower with 90 mM supplemental acetate than with the levels of 0 and 30 mM (Fig. 4A, wt and ct; α-Pta). Unlike the

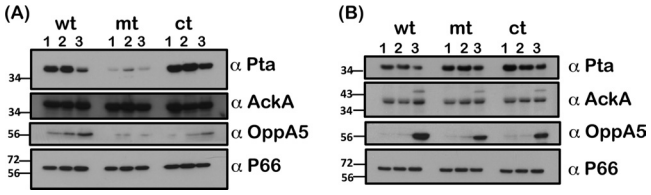

FIG 4 Immunoblot analysis of *csrA*$_{Bb}$ mutant for proteins involved in acetate metabolism. The wt, mt, and ct strains were propagated in BSK-II medium with 0 (lanes 1), 30 (lanes 2), or 90 (lanes 3) mM supplemental acetate at 23°C/pH 7.6 (A) or 37°C/pH 6.8 (B). Immunoblot analysis was done with antisera against Pta, AckA, OppA5, and P66 (loading control). Goat anti-mouse HRPO-conjugated antibodies were used as secondary antibodies and blots developed using an ECL system. Blots represent one of three independent experiments. Molecular masses in kilodaltons are indicated to the left.

mutant, the control strains had detectable increases in the levels of OppA5 at 90 mM acetate, which could contribute to increased levels of CsrA$_{Bb}$, leading to a concomitant reduction in the levels of Pta (Fig. 3 and 4; α-CsrA$_{Bb}$ and α-Pta). We did not observe any significant differences in the levels of AckA and P66, indicating equal loading of proteins and serving as an indicator that certain borrelial determinants remain unchanged under these experimental conditions.

Interestingly, when we propagated these strains at pH 6.8/37°C, we observed increased levels of Pta in the *csrA*$_{Bb}$ mutant that were independent of the levels of acetate compared to the control strains (Fig. 4B, α-Pta). Levels of Pta were detectably lower in the control strains with 90 mM acetate, while there was no difference in the levels at 0 or 30 mM acetate. There was an increased level of OppA5 in all three strains propagated with 90 mM acetate compared to 0 and 30 mM acetate (Fig. 4B, wt, mt, and ct; lanes 1 and 3, α-OppA5). Both AckA and P66 remained relatively same at pH 6.8/37°C with increasing levels of supplemental acetate. Taken together, these observations indicated that the levels of Pta could

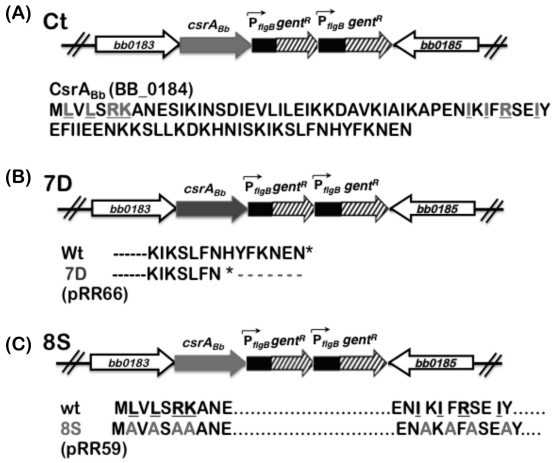

FIG 5 Schematic representation of the mutations generated in CsrA$_{Bb}$. (A) The *cis*-complemented strain (ct) was generated to restore a functional native copy of *csrA*$_{Bb}$. The residues indicated in gray are the conserved amino acids that have been shown to interact with small RNA molecule CsrB in *E. coli*. (B) Schematic representation of the DNA construct lacking the sequence encoding the last seven amino acids of CsrA$_{Bb}$ (7D). (C) Site-specific changes were made to change 8 critical residues (underlined) to alanines (8S). All three complemented strains were counterselected for resistance to gentamicin conferred by P$_{flgB}$-Gent^R.

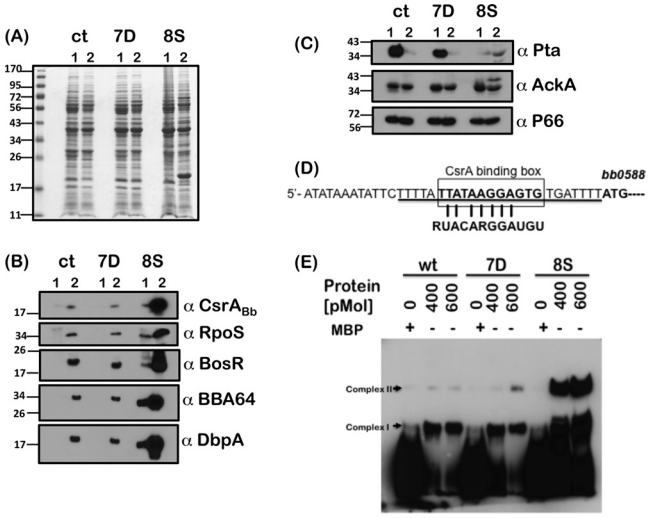

FIG 6 Phenotypic analysis of *csrA*$_{Bb}$ mutants with site-specific alterations or C-terminal deletion. (A) Proteins from *cis*-complemented strains carrying wild-type CsrA$_{Bb}$ (ct), CsrA$_{Bb}$ with a 7-amino-acid C-terminal deletion (7D), or CsrA$_{Bb}$ with substitutions of 8 critical residues (8S) were propagated under conditions mimicking the tick vector conditions before (23°C/pH 7.6) or after (37°C/pH 6.8) a blood meal. Proteins were separated on an SDS–12.5% PAGE and stained with Coomassie blue. (B) Immunoblot analysis performed with antisera against CsrA$_{Bb}$, RpoS, BosR, BBA64, and DbpA. (C) Immunoblot analysis of ct, 7D, and 8S strains with antisera against Pta, AckA, and P66 (loading control). Molecular masses in kilodaltons are indicated to the left. (D) The CsrA$_{Bb}$ binding box of the 5′UTR of *bb0588* to *bb0589* known to regulate levels of Pta was used to generate a biotinylated RNA probe (26). (E) Efficiency of binding of recombinant wt and mutant CsrA$_{Bb}$ proteins to the 5′UTR of *bb0588* to *bb0589*. A biotinylated RNA probe (20 fmol) was incubated with purified recombinant wt, 7D, and 8S fused to maltose binding protein (MBP) at the concentrations indicated above each lane. MBP alone was used at a 600-pmol concentration as a control (MBP lanes). Blots were developed using enhanced chemiluminescence (ECL) as described in Materials and Methods and represent one of three independent experiments.

be manipulated not only by altering the levels of CsrA$_{Bb}$ but also by other environmental signals such as temperature and pH and by solutes such as acetate (27).

Deletion of 7 C-terminal residues led to reduced levels of CsrA$_{Bb}$. Sequence analysis of the CsrA$_{Bb}$ revealed 7 additional C-terminal amino acids that are not present in CsrA homologs in other bacteria (34). We deleted the 7-amino-acid stretch at the C terminus (Fig. 5B) and determined the effect of this deletion in comparison with the *cis*-complemented strain carrying the wild-type *csrA*$_{Bb}$ allele. As shown in Fig. 6A, there was no apparent difference in the protein profiles of ct and 7D strains propagated at either pH 7.6/23°C (Fig. 6A, ct and 7D; lanes 1) or pH 6.8/37°C (Fig. 6A, ct and 7D; lanes 2). Immunoblot analysis with anti-CsrA$_{Bb}$ serum showed relatively lower levels of CsrA$_{Bb}$ in the 7D strain than in the ct strain under fed-tick-mimicking conditions (Fig. 6B, ct and 7D; lanes 2). This was also reflected in lower levels of RpoS, BosR, BBA64, and DbpA, indicating that the deletion of 7 amino acids caused a detectable change compared to wild-type CsrA$_{Bb}$ (Fig. 6B, ct and 7D; lanes 2). Moreover, the levels of AckA and P66 were similar in the 7D strain and the ct strain whereas the levels of Pta were lower in the 7D strain than in the ct strain at pH 7.6/23°C (Fig. 6C, ct and 7D; lanes 1). The levels of Pta were similar at pH 6.8/37°C in the two strains (Fig. 6C, ct and 7D; lanes 2). However, a notable difference that was observed was the absence

of FliW in the 7D strain compared to the *cis*-complemented strain (see Fig. 10B, α-FliW) and a significant reduction in the levels of $csrA_{Bb}$-specific transcripts compared to the ct strain (see Fig. 8).

Site-specific changes of 8 conserved residues led to increased stability of $CsrA_{Bb}$. The role of 8 key residues conserved between CsrA homologs in other bacteria and $CsrA_{Bb}$ in mediating *Borrelia*-specific functions of this regulator is unknown. We therefore employed a QuikChange site-directed mutagenesis kit to replace all 8 of the conserved residues in $CsrA_{Bb}$ (indicated in gray, Fig. 5A) that are identical in other CsrA homologs with alanines and generated a plasmid designated pRR59 with two tandem copies of P_{flgB}-GentR cloned downstream of $csrA_{Bb}$ (Fig. 5C). This plasmid was used to restore a mutant allele of $csrA_{Bb}$ in the A3-ES10 strain and counterselected with gentamicin and analyzed for levels of $CsrA_{Bb}$. To our surprise, there were increased levels of $CsrA_{Bb}$ in the 8S strain grown at pH 6.8/37°C compared to the ct strain carrying the wild-type $csrA_{Bb}$ allele (Fig. 6B, ct and 8S; lanes 2, α-$CsrA_{Bb}$). The increased levels of $CsrA_{Bb}$ in the 8S strain also resulted in increased levels of RpoS, BosR, BBA64, and DbpA (Fig. 6B, 8S; lane 2) as well as OspC (Fig. 6A, 8S; lane 2) compared to the ct strain (Fig. 6B, ct; lane 2). We also observed that there were detectable levels of $CsrA_{Bb}$ in the 8S strain that correlated with increased levels of RpoS, BosR, BBA64, and DbpA even under conditions mimicking those seen in unfed ticks (Fig. 6B, ct and 8S; lanes 1). If the levels of acetyl phosphate are critical for activation of the Rrp2-RpoN-RpoS pathway, we expected the levels of Pta to be repressed to a greater extent in the 8S mutant than in the ct strain, resulting in increased levels of RpoS and *rpoS*-regulated proteins. Consistent with this expectation, the Pta levels were much lower in the 8S mutant under unfed-tick conditions compared to the ct strain levels, thereby contributing sufficient acetyl phosphate for increased activation of the *rpoS* regulon (Fig. 6C, ct and 8S; lanes 1). However, under fed-tick conditions, the levels of Pta in the ct and 8S strains were similar (Fig. 6C, 8S; lane 2). One additional difference is the significantly higher levels of *pta* transcripts in the 8S than in the ct strain that are regulated by increased levels of $CsrA_{Bb}$, resulting in similar levels of Pta (protein) under fed-tick conditions (see Fig. 8). We also observed a higher-molecular-mass protein that reacted with anti-AckA antibodies in the 8S strain compared to the ct strain, while the levels of P66 were similar in these strains (Fig. 6C, ct and 8S; α-AckA and α-P66). Taken together, these observations indicate enhanced stability of the 8S mutant $CsrA_{Bb}$ protein with functional integrity to regulate Pta in *B. burgdorferi*.

$CsrA_{Bb}$ with an 8-amino-acid substitution (8S) binds the 5′UTR of *pta*. EMSA with a biotinylated RNA probe corresponding to the 5′UTR of *pta* performed with wild-type, 7D, and 8S CsrABb protein revealed binding to the labeled riboprobes (complex 1), while there was no binding to MBP alone (Fig. 6D) (26). However, increased levels of complex 1 and complex 2 indicated that the ability of the 8S $CsrA_{Bb}$ mutant protein to bind to the 5′UTR of *pta* was higher than that of the parental or 7D mutant $CsrA_{Bb}$ proteins (Fig. 6E). There no shift in the mobility of the RNA probes when purified MBP alone was used in the reactions, indicating that the complex formation was due to the specific binding of $CsrA_{Bb}$ proteins to the RNA probe.

Levels of acetyl-CoA are lower in the 8S mutant. We also observed that the levels of acetyl-CoA were significantly lower in the 8S strain under unfed-tick-specific conditions than in the ct and 7D strains (Fig. 7). These levels reflect the increased levels of Pta

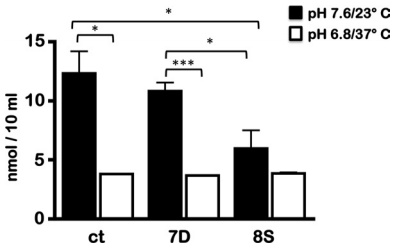

FIG 7 Levels of acetyl-CoA accumulation in mutant $csrA_{Bb}$ strains. Borrelial strains (ct, 7D, and 8S) were propagated at 23°C/pH 7.6 (black bars) and 37°C/pH 6.8 (open bars) to densities of approximately 5×10^7 cells/ml and 1×10^8/ml, respectively. Lysates were prepared from a total of 10^9 spirochetes using perchloric acid, and levels of acetyl-CoA in the extracts were analyzed using a PicoProbe acetyl-CoA assay kit and Student's *t* test implemented in Prism software. Asterisks indicate levels of significance (***, $P < 0.001$; *, $P < 0.05$).

observed in the ct and 7D strains at pH 7.6/23°C (Fig. 6C; lane 1, α-Pta) compared to the 8S strain, confirming the ability of the $CsrA_{Bb}$ 8S mutant protein to repress Pta expression under unfed-tick conditions where it is present in detectable amounts (Fig. 6C, 8S; lane 1, α-Pta). The levels of acetyl-CoA, however, under the fed-tick conditions (Fig. 7, pH 6.8; 37°C) were similar in all three strains, reflecting the effect of similar levels of Pta under these conditions (Fig. 6B, lane 2, α-Pta). These observations indicate that the levels of Pta regulated by $CsrA_{Bb}$ largely determine the levels of acetyl-CoA accumulation in *B. burgdorferi*.

Transcriptional changes in the 7D and 8S mutants. Since immunoblot analysis of the 7D and 8S mutant strains revealed reduced and increased levels of $CsrA_{Bb}$, respectively, compared to the ct strain levels, we accessed if these differences were due to transcriptional levels of $csrA_{Bb}$. We isolated total RNA from the ct, 7D, and 8S strains at pH 6.8/37°C where $CsrA_{Bb}$ levels are maximal to determine its effects in regulating a subset of linked and distal ORFs. We focused on determining if changes in $csrA_{Bb}$ levels altered the transcriptional levels of members of the *flgK* motility operon and on two distal ORFs, *flaB* and *pta*. As shown in Fig. 8, quantitative RT-PCR revealed that there was a significant reduction ($P < 0.05$) in the levels of $csrA_{Bb}$ transcripts in the 7D strain compared to those in the ct strain carrying the parental copy of $csrA_{Bb}$. The transcript levels of $csrA_{Bb}$ were significantly higher in the 8S strain, which is consistent with what was observed at the protein level ($P < 0.001$). Compared to those of the ct strain, the levels of the divergently transcribed ORF *bb0185*, downstream of $csrA_{Bb}$, were significantly upregulated in the 7D strain, while the opposite was true in the 8S strain. Transcription of the ORF upstream of $csrA_{Bb}$, *bb0183* (*fliW*) was elevated in the 8S strain compared to the ct and 7D strains ($P < 0.001$), while there was a less significant difference ($P < 0.1$) between the ct and 7D strains in the levels of *bb0183*. Notably, the transcriptional levels of *flaB* were significantly reduced in the 7D and 8S strains compared to the ct strain (Fig. 8). Moreover, the levels of the cotranscribed *bb0588* to *bb0589* ORFs were significantly higher in the 7D and 8S strains than in the ct strain whereas a similar trend was observed with transcripts specific to *pta* alone (*bb0589*) in these strains. It should be noted that while the transcriptional levels of *bb0588* to *bb0589* and *bb0589* (*pta*) were elevated in the 7D and 8S strains compared to the control strain, the levels of Pta are regulated at the protein level posttranscriptionally and are significantly different in the ct and 7D strains from those in the 8S strain (Fig. 6C, α-Pta).

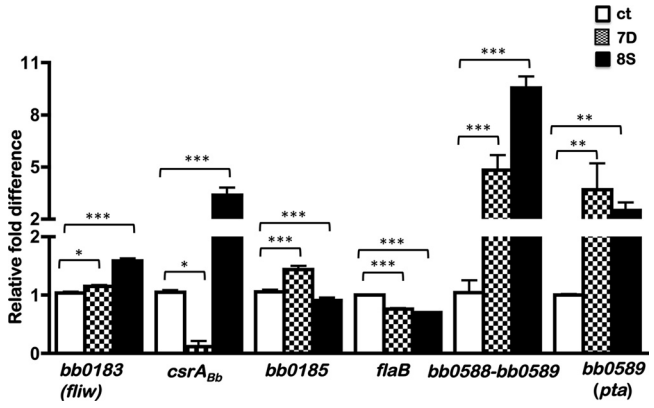

FIG 8 Real-time reverse transcription-PCR analysis of levels of select ORFs in the ct, 7D, and 8S strains. Total RNA was isolated from borrelial strains propagated at pH 6.8/37°C as described in Materials and Methods and subjected to reverse transcription-PCR. The values for all the samples were normalized relative to the value for *recA*, and the change in the C_T value for each transcript was obtained as an average of the values determined for each sample analyzed in triplicate. The $2^{-\Delta\Delta CT}$ values for each transcript from the ct, 7D, and 8S strains are shown as fold difference on the *y* axis with corresponding error bars. The ΔC_T values obtained for all the ORFs analyzed from each borrelial strain were subjected to an unpaired Student's *t* test implemented in Prism software. The asterisks indicate levels of significance as follows: ***, $P < 0.001$; **, $P < 0.01$; *, $P < 0.05$.

Increased acetate alters the phenotype of 7D and 8S mutants. We determined if increasing levels of supplemental acetate would alter the levels of Pta in the ct, 7D, and 8S strains at either pH 7.6/23°C (Fig. 9A and B) or pH 6.8/37°C (Fig. 9C and D). The levels of Pta were significantly lower in the 8S strain than in strain ct or strain 7D at pH 7.6/23°C (Fig. 9B, 8S; lanes 1 to 3). While OppA5 was elevated in all three strains with the highest levels of supplemental acetate (Fig. 9B, lanes 3), the levels of AckA and P66 were similar in all three strains (Fig. 9B). The increased levels of OspC were also observed in samples propagated with 90 mM acetate in all three strains at pH 7.6/23°C (Fig. 9A, ct, 7D, and 8S; lanes 3). However, the levels of Pta were significantly higher in the 7D than in the ct strain at pH 7.6/23°C with increasing concentrations of supplemental acetate (Fig. 9B, ct and 7D; lanes 1 to 3, α-Pta). The higher levels of 8S CsrA$_{Bb}$ mutant protein under unfed-tick-specific conditions could contribute to the observed lower levels of Pta in the 8S strain than in the ct and 7D strains (Fig. 6B; lane 1, α-CsrA$_{Bb}$).

When the ct, 7D, and 8S strains were propagated at pH 6.8/37°C, the Pta levels were relatively unchanged with increasing concentrations of acetate in each of these strains (Fig. 9D, α-Pta). In addition, the levels of Pta in the 7D mutant were higher than in the ct and 8S strain (Fig. 9D; 7D, α-Pta), coinciding with lower levels of CsrA$_{Bb}$ at both the transcriptional and translational levels than in the ct or 8S strain (Fig. 8 and 6B, α-CsrA$_{Bb}$). Another notable difference between these strains was the levels of OppA5 in the 8S strain (Fig. 9D, 8S, α-OppA5). While OppA5 was detectable in the ct and 7D strains exposed to 90 mM acetate (Fig. 9B, ct and 7D; lanes 3), the levels of OppA5 in the 8S strain were consistently higher with increasing concentrations of supplemental acetate. The increase in OppA5 levels also coincided with a noticeable reduction in the levels of Pta in the 8S strain when propagated with increasing concentrations of acetate (Fig. 9D, 8S; lane 3, α-Pta). Collectively, these observations indicate that both CsrA$_{Bb}$ and the intracellular levels of acetate affect the Pta levels and in the process contribute to the activation of the Rrp2-RpoN-RpoS pathway.

FlaB levels in *csrA$_{Bb}$* deletion and site-specific mutant strains. There were minimal differences in the levels of FlaB in the mt and ct strains grown at pH 7.6/23°C compared to growth at pH 6.8/37°C (Fig. 10A, mt and ct; α-FlaB), while the wt strain had approximately 1.5 times more FlaB under unfed-tick-mimicking conditions (Fig. 10A, wt; lane 1, a-FlaB). This suggested that the effect of regulation of FlaB by *csrA$_{Bb}$* expressed as part of the *flgK* motility operon was subtle under the growth conditions employed in this study. This is in contrast to what has been observed when *csrA$_{Bb}$* was expressed either constitutively or inducibly at higher levels in *trans* using a borrelial shuttle vector or under growth conditions that were distinct from this study (26, 28, 41). There were no dramatic differences in the levels of FlaB in the ct, 7D, and 8S strains under both unfed- and fed-tick-mimicking conditions, even though the levels of mutant CsrA$_{Bb}$ protein in the 8S strain were dramatically higher than in the ct and 7D strains. It appears that the replacement of 8 key residues with alanines in CsrA$_{Bb}$ increased its posttranscriptional effect on *pta* but does not have an effect with regard to the regulation of *flaB*. Alternatively, since the mutant CsrA$_{Bb}$ proteins were synthesized in *cis*, the coordinated synthesis with other members of the *flgK* motility operon could potentially circumvent its effect on the *flaB* transcripts.

FliW is downregulated in CsrA$_{Bb}$ and the 7D mutant. We hypothesized that the presence of 7 additional amino acids at the C terminus of CsrA$_{Bb}$ would provide clues to the function of this regulator that are unique to the pathophysiology of *B. burgdorferi*. Our initial analysis of 7D strain revealed a decrease in the levels of CsrA$_{Bb}$, RpoS, BosR, and select members of the *rpoS* regulon when grown at pH 6.8/37°C (Fig. 6A and B). While the levels of *bb0183* (*fliW*) were elevated only modestly in the transcriptional analysis, we decided to determine if CsrA$_{Bb}$ levels affected FliW. Immunoblot analysis showed that there was no detectable FliW in the *csrA$_{Bb}$* mutant at both 7.6/23°C and 6.8/37°C compared to the wt or ct strain (Fig. 10A, wt, mt, and ct; α-FliW). Interestingly, we

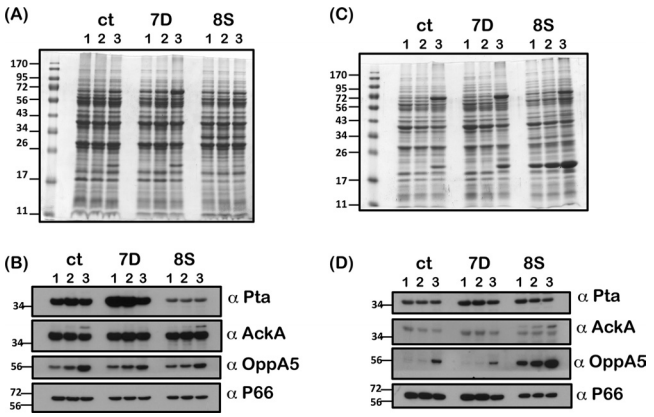

FIG 9 Immunoblot analysis of ct, 7D, and 8S mutant strains of *B. burgdorferi* grown with supplemental acetate. Total proteins from ct, 7D, and 8S strains were grown under unfed (23°C/pH 7.6) (A and B) or fed (37°C/pH 6.8) (C and D) tick conditions with 0 (lanes 1), 30 (lanes 2), and 90 (lanes 3) mm of supplemental acetate. Equivalent amounts of proteins were separated on an SDS–12.5% PAGE gel (A and B). Separated proteins were electrotransferred and subjected to immunoblot analysis (B and D) using antisera against Pta, AckA, OppA5, and P66 (loading control). Blots represent one of three independent experiments. Molecular masses in kilodaltons are indicated to the left.

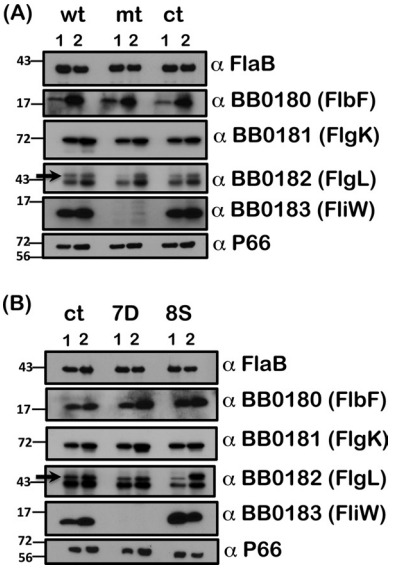

FIG 10 Effect of $CsrA_{Bb}$ on the members of the *flgK* motility operon. Separated proteins of strains wt, mt, and ct (A) and strains ct, 7D, and 8S (B) propagated under conditions that mimic the tick midgut before (23°C/pH 7.6; lanes 1) and after (37°C/pH 6.8; lanes 2) a blood meal were electrotransferred and subjected to immunoblot analysis using antisera against FlaB, BB0180 (FlbF), BB0181 (FlgK), BB0182 (FlgL, indicated by arrow), BB0183 (FliW), and P66 (loading control). Note the absence of any detectable levels of FliW in the $csrA_{Bb}$ mutant and 7D strain. Levels of FliW were elevated in the 8S mutant compared to the ct strain under unfed-tick conditions. Levels of FlbF and FlgK were unchanged in the strains tested. Blots represent one of two independent experiments. Molecular masses in kilodaltons are indicated to the left.

also noted that the levels of FliW in the 7D strain were similar to the $csrA_{Bb}$ mutant levels, suggesting that the lack of 7 C-terminal residues was sufficient to reduce the levels of FliW to that observed in the $csrA_{Bb}$ mutant (Fig. 10B, 7D; α-FliW). In addition, we observed increased levels of FliW in the wt and ct strains under fed-tick-mimicking conditions, where the levels of $CsrA_{Bb}$ were higher (Fig. 10B, wt, ct, and 8S; lanes 2). The levels of FliW were increased in the 8S mutant grown under both growth conditions, even though the FliW levels were relatively higher under unfed-tick-mimicking conditions (Fig. 10B, 8S; lanes 1 and 2, α-FliW). Immunoblot analysis of levels of synthesis of other members of the *flgK* motility operon such as FlbF, FlgK, and FlgL revealed no significant changes between the wt, mt, and ct strains and between the ct, 7D, and 8S mutants.

$CsrA_{Bb}$ binds to the upstream region of *fliW*. Sequence analysis of regions of *flgK* motility operon helped identify two potential $CsrA_{Bb}$ binding sites (consensus sequence, RUACARGGA UGU) located upstream of *fliW* (Fig. 11A, B, and C). The consensus $CsrA_{Bb}$ binding sites were located within the *flgK* coding sequence (Fig. 11A). *B. burgdorferi* strains B31 and ZS7 had identical binding sequences, while *B. afzelli* PKo and *B. garinii* PBi had a nucleotide difference in the BS2 site (Fig. 11B). EMSA revealed binding of $rCsrA_{Bb}$ to biotinylated RNA probes containing both binding sites (BS1 and BS2) upstream of *fliW*, while there was no binding to RNA probes mutated at both binding sites (Fig. 11D). Moreover, there was reduced binding of $rCsrA_{Bb}$ with RNA probes spanning either BS1 or BS2 individually. These studies indicated that there are additional regulatory modules that interact with $CsrA_{Bb}$ in the 5′UTR of *fliW* and $csrA_{Bb}$. Since the translational levels of FlbF, FlgK, and FlgL in the parental and mutant strains are similar, it is possible that a second transcript with regulatory modules containing $CsrA_{Bb}$ binding sites could account for the differences in the levels of FliW and $CsrA_{Bb}$ in the mt, 7D, and 8S strains. In summary, levels of $CsrA_{Bb}$ appear to have a direct effect on the levels of FliW and on its own synthesis.

DISCUSSION

The molecular mechanisms that contribute to the adaptation of *B. burgdorferi* are key to its ability to survive in the tick vector or vertebrate host (2, 3, 52). Recent advances in the regulation of this adaptive process using targeted deletion mutants have expanded our understanding of the integration of multiple external signals and interplay of several regulatory molecules (2, 24, 53–58). Among them, $CsrA_{Bb}$ plays a crucial role in coupling the metabolic status of the *B. burgdorferi* to gene expression profiles specific to its host by regulating the levels of Pta, among others, which in turn determines the intracellular levels of a key activation molecule, acetyl phosphate (23, 26, 27). The effects of the connection between the conserved and unique residues of $CsrA_{Bb}$ with respect to its pathogen-specific function, its location on the borrelial chromosome as a terminal ORF of a large motility operon, and its ability to modulate pathogenesis-related proteins by regulating acetate transport and utilization via OppA5, AckA, and Pta are not completely understood. We therefore explored the molecular basis of the location/structure of $CsrA_{Bb}$ with respect to its functions and determined (i) the effect of $CsrA_{Bb}$ and acetate levels on Pta; (ii) the contributions of key residues to the functions of $CsrA_{Bb}$; and (iii) the effect of $CsrA_{Bb}$ on the proteins associated with *flgK* motility operon of *B. burgdorferi*.

(i) Effect of $CsrA_{Bb}$ and acetate levels on Pta. $CsrA_{Bb}$ directly represses *pta* posttranscriptionally, leading to accumulation of acetyl phosphate, which in turn serves to activate the Rrp2-RpoN-RpoS pathway (26). The validity of this notion is borne out by the observation that even when transcriptional levels of *pta* are high, under conditions where levels of $CsrA_{Bb}$ are elevated, translational levels of Pta are significantly reduced (Fig. 6C and 8). The functional effects of Pta are also reflected in lower levels of acetyl-CoA (Fig. 7). However, there was no drastic increase in the level of Pta in the $csrA_{Bb}$ mutant, suggesting the possibility of dissociation between the transcriptional and posttranscriptional regulatory effects of *pta*. When we exposed the $csrA_{Bb}$ mutant to increased levels of acetate, there was restoration of RpoS and *rpoS*-regulated proteins to the levels observed in the control strains. These observations provided a connection between the levels of acetate, effects of $CsrA_{Bb}$, and the transcriptional and translational levels of Pta, demonstrating a link between the metabolic status of the spirochetes and its host-specific adaptation. Moreover, these findings provided clues to the signals needed to optimize the gene expression profiles to facilitate the adaptation of *B. burgdorferi* to a multitude of hosts.

It should be noted that even though there is significant sequence similarity between the borrelial and other bacterial CsrA homologs, the regulation of Pta by $CsrA_{Bb}$ appears to be uniquely important, as there is no apparent homolog(s) of acetyl-coenzyme A synthetase (Acs) present in *B. burgdorferi* that could also contribute to the generation of a critical metabolic intermediate acetyl-CoA (34, 59, 60). Acs present in several bacterial species such as *Escherichia coli* is positively regulated by CsrA, and BLASTP analysis of the borrelial proteome

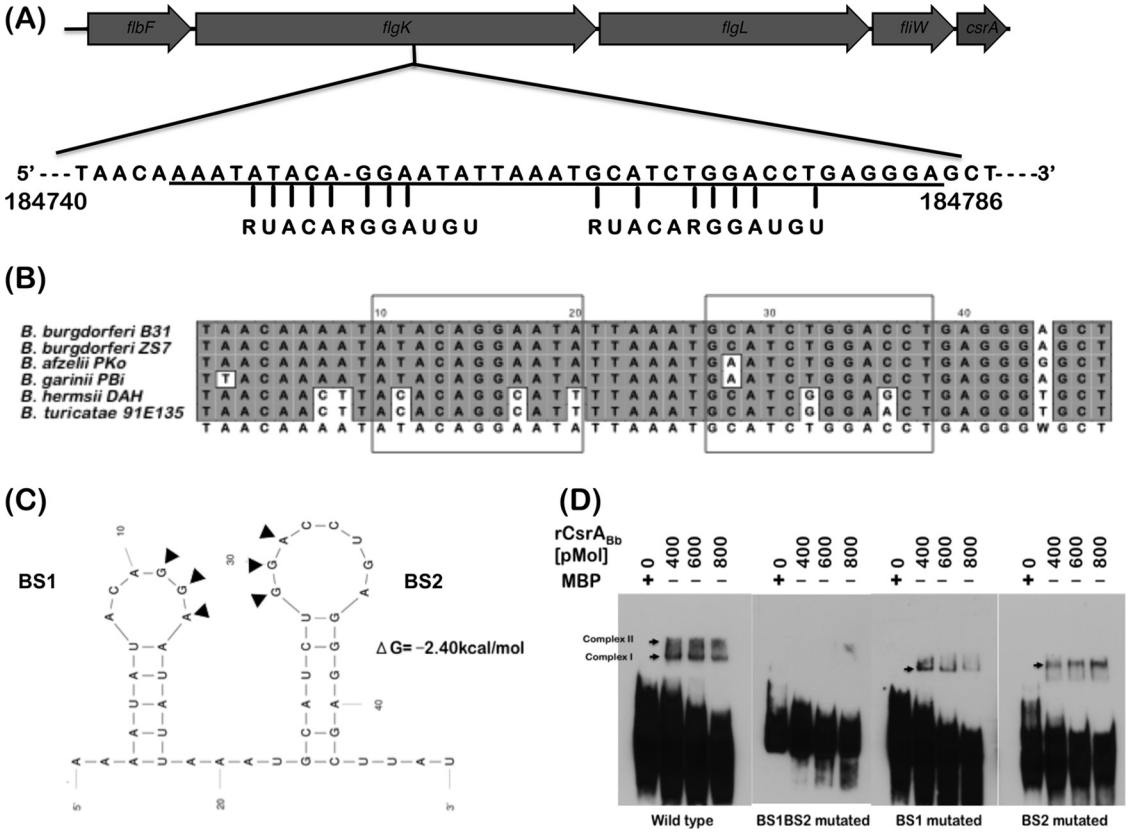

FIG 11 $CsrA_{Bb}$ binding sites upstream of FliW. (A) The sequence upstream of *fliW* was analyzed for potential $CsrA_{Bb}$ binding domains, and two putative domains were identified within the coding sequence of *flgK*. (B) Sequenced borrelial strains were analyzed for the presence of $CsrA_{Bb}$ binding domains, and *B. burgdorferi* strains B31 and ZS7 have identical sequences in these domains, while *B. afzelii* Pko and *B. garinii* PBi have one nucleotide difference in the second domain. Additional differences in the sequences in the relapsing fever borreliae have been observed in this analysis. (C) Mfold program was used to generate the secondary structure and free-energy values of the two binding sites of $CsrA_{Bb}$ in the upstream region of *fliW*. Arrows indicate a conserved CsrA binding nucleotide at each site. (D) Efficiency of binding of recombinant $CsrA_{Bb}$ to RNA probes corresponding to BS1 and BS2. A biotinylated RNA probe (20 fmol) was incubated with purified recombinant $CsrA_{Bb}$ fused to maltose binding protein (MBP) at the concentrations indicated above each lane. MBP alone was used at a 600-pmol concentration as a control (MBP lane). Mutated probes with replacement of GGA>AAA at either or both of the two binding sites were used as indicated below the blots. Blots were developed using enhanced chemiluminescence (ECL) as described in Materials and Methods. Blots represent one of three independent experiments.

for an Acs homolog(s) matched only long-chain-fatty-acid CoA ligases (BB0137 [$3.9e^{-15}$], BB0593 [$2.4e^{-08}$]). Therefore, the functions of $CsrA_{Bb}$ within the context of the borrelial pathophysiology appear to be unique and warrant further characterization since the levels of acetyl-CoA, which serves as the initial substrate for central metabolic pathways affecting cell wall biogenesis and other physiological processes, are determined at least in part by the regulatory effects of $CsrA_{Bb}$ (27).

It is also interesting that there could be a potential feedback loop connecting the levels of $CsrA_{Bb}$, OppA5, and Pta (27, 29, 33). This hypothesis is based on several lines of evidence. For example, we noted that when *oppA5* was deleted, there was a reduction in the levels of $CsrA_{Bb}$, RpoS, and several members of the *rpoS* regulon (33). Under conditions favoring increased levels of OppA5, we observed increased levels of those regulators and the opposite was true when $CsrA_{Bb}$ was deleted, suggesting a potential link between the functions of $CsrA_{Bb}$ and OppA5 (29).

The effect of the supplementation of acetate on ct, 7D, and 8S strains resulted in levels of Pta that were consistent with expected phenotypes of these strains. For example, in spite of the increase in the levels of acetate, the Pta levels were lower in the 8S strain than in the ct or 7D strains due to the posttranslational repression of *pta* mediated by 8S mutant $CsrA_{Bb}$ protein at pH 7.6/23°C (Fig. 9B). However, the reduced levels of $CsrA_{Bb}$ observed in the ct and 7D strains noted under these growth conditions resulted in increased Pta levels (Fig. 9B). In addition, the levels of OppA5 in the 8S strain with no acetate supplementation were elevated, indicating that increased or stable levels of $CsrA_{Bb}$ contribute to this phenotype (Fig. 9D, 8S; α-OppA5). Our phenotypic analysis of the deletion- and site-specific mutants, levels of acetyl-CoA in some of these strains, and kinetics of binding of various $CsrA_{Bb}$ proteins to the 5′UTR of *pta* have indicated that the levels of acetate, the transcriptional levels of *pta*, and posttranscriptional regulation of *pta* by $CsrA_{Bb}$ determine the balance between the acetyl phosphate and acetyl-CoA levels to sustain or dampen the activation of the Rrp2-RpoN-RpoS pathway modulating adaptation of the spirochetes to the vertebrate host. The initiating point of the loop and/or if other signals/mediators interface with this loop remains to be determined.

(ii) Functional contributions of key residues of $CsrA_{Bb}$. To further identify the regulatory mechanism of $CsrA_{Bb}$, we analyzed borrelial mutants with 8 conserved residues replaced with alanines

(in gray; Fig. 5A) or lacking 7 C-terminal amino acids unique to the borrelial CsrA homolog (36). While the 8S mutant resulted in a stable $CsrA_{Bb}$ mutant protein that was capable of binding to the 5′UTR of *pta*, the 7D mutant appears to have a less stable $CsrA_{Bb}$ protein. If the structure and function of $CsrA_{Bb}$ were akin to the solved structures of 3 CsrA homologs that function as homodimers, the 7-residue C-terminal part of $CsrA_{Bb}$ might provide the critical interaction domain from each monomer along with the N-terminal domain to form the functional region interacting with its cognate RNA molecules (36). Deletion of this domain could reduce the stability of either the transcript or translated products. Consistent with this expectation, we did see a reduction in the transcriptional levels of $csrA_{Bb}$ in the 7D strain even though there was only a small reduction in the levels of synthesis of 7D $CsrA_{Bb}$ protein compared to the ct strain. The overall effects of 7D protein on the posttranscriptional regulation of *pta* were similar to those seen with the ct strain even though there was a weak "supershift" noted with the recombinant 7D protein, indicating binding to the labeled riboprobe corresponding to the 5′UTR of *pta*. Based on these observations, the absence of 7 C-terminal residues results in a lower levels of $CsrA_{Bb}$ even though the ability to bind to *pta* is still intact. The contribution of each of the 7 C-terminal residues to the stabilization of $CsrA_{Bb}$ protein remains to be determined.

We anticipated that the replacement of 8 key residues with alanines would abolish the function of $CsrA_{Bb}$. However, we observed that the levels of $CsrA_{Bb}$ and several proteins such as RpoS, BosR, BBA64, and DbpA were upregulated in the 8S strain compared to the ct strain carrying the wild-type $csrA_{Bb}$ allele, suggesting a potential stabilization of the 8S mutant $CsrA_{Bb}$ transcript and protein (Fig. 6 and 8, ct and 8S). The replacement of these residues did not alter the function of $CsrA_{Bb}$ but rather elevated its effects. Specifically, the ability of 8S mutant protein to bind and regulate *pta* posttranscriptionally was significantly higher than that seen with the parental $CsrA_{Bb}$ as revealed by EMSAs (Fig. 6E, complex 2), immunoblot analysis using anti-Pta serum (Fig. 6C, 8S), and reduced levels of acetyl-CoA at 23°C/pH 7.6 (Fig. 7, 8S). The increased stability of $CsrA_{Bb}$ also resulted in higher transcript and protein levels of FliW (*bb0183*) (Fig. 8, 10B). This suggested the overall stability of the cotranscribed product (e.g., *fliW-*$csrA_{Bb}$), resulting in higher levels of the respective translated products. The phenotype observed with the 8S strain is partly similar to that of *E. coli* carrying CsrA with arginine-to-alanine substitutions at positions 6 and 44 (R6A and R44A), respectively, which resulted in increased stabilization of the protein due to reduced proteolysis or formation of aggregates (36). However, unlike the functional impairment observed with these mutant CsrA proteins in *E. coli*, R6A and R44A substitution in conjunction with those of 6 other amino acids enhanced several functions of $CsrA_{Bb}$ in the 8S strain. Taken together, our observations demonstrate that the replacement of 8 conserved residues of $CsrA_{Bb}$ appears to have stabilized the $CsrA_{Bb}$ transcript and/or the protein and in the process enhanced its regulatory functions. Of note, it is possible that the changes in multiple conserved residues could compensate for loss or alteration of functions mediated by individual residues. Due to the inherent difficulties in generating mutant strains of *B. burgdorferi*, we decided to generate a mutant strain with changes in all 8 conserved residues in $CsrA_{Bb}$ to verify the phenotype rather than focus on generating mutant strains with changes in each of the conserved residues. Our genetic analyses of 7D and 8S strains have expanded our understanding of the conserved and pathogen-specific effects of $CsrA_{Bb}$ and that those effects are largely dependent on the phenotypes of the *cis*-complemented (ct) strain carrying the parental $csrA_{Bb}$ with identical copies of antibiotic selection markers.

(iii) Effect of $CsrA_{Bb}$ on the proteins associated with motility of *B. burgdorferi*. We observed a 1.5-fold increase in FlaB levels in the parental strain, B31-A3, propagated under unfed-tick conditions (pH 7.6/23°C) compared to fed-tick conditions (pH 6.8/37°C) (Fig. 10A, wt; lanes 1 and 2, α-FlaB). A similar, albeit less pronounced, effect on the FlaB levels was observed when the mt was propagated under these two different growth conditions. This suggests that additional unknown factors/signals contribute to the levels of FlaB. Previously, it has been shown that the absence of $csrA_{Bb}$ resulted in a 4-fold increase in the levels of FlaB compared to the parental strain levels even though the levels of *flaB* transcripts were relatively the same in both the strains, indicating $CsrA_{Bb}$-mediated posttranscriptional regulation of FlaB (26, 28, 41). While we did not observe such drastic increases in the levels of FlaB in our $csrA_{Bb}$ mutant generated using the same parental strain (B31-A3), our growth conditions were different from the previous study, and that could partly explain the difference in this phenotype. Both the 7D and 8S strains did not exhibit significant changes in the levels of FlaB even though these mutant $CsrA_{Bb}$ proteins had significant differences in their ability to interact with the 5′UTR of *pta* and *fliW*. We propagated the strains under conditions mimicking the tick midgut before or after a blood meal with CO_2 levels maintained constantly at 1%, whereas the levels of FlaB measured in the previous study resulted from the use of lysates from strains propagated at 34°C with 3.4% CO_2 levels (26, 41, 44, 45, 47, 49). Moreover, the complex nature of the borrelial growth medium, BSK-II, could also contribute to variations in the levels of a multitude of signals/nutrients that may have a direct or indirect effect on FlaB levels that is independent of $CsrA_{Bb}$ levels. Past studies from our own laboratory also showed that $CsrA_{Bb}$ levels affected the accumulation of FlaB notably when $csrA_{Bb}$ was expressed in *trans* from a shuttle vector under the control of the constitutive promoter, P_{flgB} (28). The latter observation indicated that since $CsrA_{Bb}$ is the terminal ORF of the *flgK* motility operon, coordinated synthesis of proteins from this operon might provide a critical balance for optimizing FlaB levels. Also, if $CsrA_{Bb}$ was synthesized without synchronization with the other members of the *flgK* motility operon following in *trans* expression from a shuttle vector, it could have additional distal effects. Consistent with this observation, when we expressed $CsrA_{Bb}$ in *cis*, the levels of FlaB in the ct strain were similar to the wt strain levels. Recently, it has been documented that complementation in *trans* could lead to overexpression of the protein either due to the copy number of the shuttle vector or due to the absence of regulatory effects from upstream elements that may not be included in the *trans*-complementing plasmids (61). Interestingly, when we expressed the mutant allele of $csrA_{Bb}$ (8S) that resulted in the elevated levels of $CsrA_{Bb}$, there was no drastic alteration in the levels of FlaB compared to the ct or 7D strain levels (Fig. 10B, α-FlaB). It is possible that the changes in 8S $CsrA_{Bb}$ mutant protein resulted in an inability to regulate *flaB* whereas it did retain its regulatory effects on *pta*. Nevertheless, these findings indicate the contributions of key residues in modulating different functions of $CsrA_{Bb}$. Taken together, these observations indicate that $CsrA_{Bb}$ can differentially regulate the levels of expression of proteins critical for motility/

morphology as well as proteins critical for adherence (e.g., DbpA, BBK32, etc.). This is critical in facilitating the adaptation of *B. burgdorferi* to specific microenvironments where motility or adherence may acquire importance. These regulatory aspects of $CsrA_{Bb}$ are unique to the pathophysiological response of *B. burgdorferi* and exhibit interesting deviations from the effects mediated by $CsrA_{Bb}$ in other Gram-negative bacteria, such as *E. coli* or *Salmonella*, where the levels of the small RNA *csrB* or *csrC* rather than the levels of CsrA largely determine the signal-dependent adaptive responses (62).

Recently, the contribution of FliW as a protein antagonist of CsrA activity has been demonstrated in *B. subtilis* (38, 40). FliW released from the FliW-Hag (flagellin) complex following the secretion of flagellin titrates out CsrA, thereby removing the translational repression of *hag* mediated by CsrA. This occurred concurrently with flagellin assembly, providing a mechanism where the flagellin homeostatically regulates itself. Since the ORF upstream of $CsrA_{Bb}$ (*bb0184*) is FliW (*bb0183*), we hypothesized that the levels of FliW could affect the functions of $CsrA_{Bb}$. We observed that FliW was not detectable in the $csrA_{Bb}$ mutant and 7D strains whereas the levels of FliW were elevated in the 8S strain (Fig. 10A and B, α-BB0183). Even though FliW was undetectable at the protein level in the 7D strain, there were no significant differences in the levels of *fliW* (*bb0183*) transcripts in the ct and 7D strains, indicating that $CsrA_{Bb}$ regulates *fliW* levels posttranscriptionally (Fig. 8). While the levels of FliW were higher under the fed-tick conditions in strains wt and ct, its level was elevated under unfed-tick conditions in the 8S mutant, suggesting that additional signals could come into play in determining levels of FliW (Fig. 10A and B, wt, ct, and 8S; lanes 2, α-BB0183).

Sequence analysis of the upstream region of *fliW* revealed the presence of conserved CsrA binding domains that formed two stem-loops, with conserved GGA motifs within the loops (Fig. 11A and C). The sequences corresponding to these stem-loops were identical in the sequenced strains of *B. burgdorferi* and appear to be fairly well conserved in other related borrelial strains (Fig. 11B). EMSAs demonstrated that recombinant $CsrA_{Bb}$ was able to bind to the riboprobes corresponding to these regions, and replacement of the conserved GGA residues resulted in reduced or no binding to the target probes. Based on these observations, it appears that $CsrA_{Bb}$ positively regulates FliW. However, the effects of FliW on $CsrA_{Bb}$ and the downstream effects of these potential interactions remain to be determined. Immunoblot analysis for levels of other members of the *flgK* motility operon indicated no major differences in the levels of BB0180 (FlbF) and BB0181 (FlgK), while there were subtle changes in the levels of BB0182 (FlgL) in the deletion and site-specific mutants of $CsrA_{Bb}$ (Fig. 10A and B).

In summary, $CsrA_{Bb}$ contributes not only to the activation of the pathway critical for adaptation to the vertebrate host but also to regulating key proteins, notably members of the *flgK* motility operon, involved in motility/morphology. These studies demonstrate a versatile role for $CsrA_{Bb}$ in regulating several aspects of the pathophysiology of *B. burgdorferi*. Further studies on how $CsrA_{Bb}$ is activated in different niches occupied by *B. burgdorferi* will help devise strategies to regulate $CsrA_{Bb}$ and thereby reduce the adaptive capabilities or virulence of *B. burgdorferi*, leading to a reduction in the incidence or severity of Lyme disease.

ACKNOWLEDGMENTS

We thank Patti Rosa for *B. burgdorferi* strain B31-A3 and Darrin R. Akins for the anti-BBA64 serum.

This study was partly supported by Public Health Service grant SC1-AI-078559 from the National Institute of Allergy and Infectious Diseases, the Army Research Office of the Department of Defense under contract W911NF-11-1-0136, a predoctoral fellowship from the South Texas Center for Emerging Infectious Diseases (STCEID) to S.L.R.K. and Y.-H.L., and a predoctoral fellowship from the Center of Excellence in Infection Genomics (CEIG) to C.L.M.

The funders had no role in the study design, data collection, and analysis, the decision to publish, or the preparation of this article.

REFERENCES

1. **Barbour AG.** 1989. The molecular biology of Borrelia. Rev. Infect. Dis. **11**(Suppl)6:S1470–S1474.
2. **Samuels DS.** 2011. Gene regulation in *Borrelia burgdorferi*. Annu. Rev. Microbiol. **65:**479–499.
3. **Radolf JD, Caimano MJ, Stevenson B, Hu LT.** 2012. Of ticks, mice and men: understanding the dual-host lifestyle of Lyme disease spirochaetes. Nat. Rev. Microbiol. **10:**87–99.
4. **Miller CL, Karna SL, Seshu J.** 2013. Borrelia host adaptation Regulator (BadR) regulates *rpoS* to modulate host adaptation and virulence factors in *Borrelia burgdorferi*. Mol. Microbiol. **88:**105–124.
5. **Babb K, El-Hage N, Miller JC, Carroll JA, Stevenson B.** 2001. Distinct regulatory pathways control expression of *Borrelia burgdorferi* infection-associated OspC and Erp surface proteins. Infect. Immun. **69:**4146–4153.
6. **Brooks CS, Hefty PS, Jolliff SE, Akins DR.** 2003. Global analysis of *Borrelia burgdorferi* genes regulated by mammalian host-specific signals. Infect. Immun. **71:**3371–3383.
7. **Crowley JT, Toledo AM, LaRocca TJ, Coleman JL, London E, Benach JL.** 2013. Lipid exchange between *Borrelia burgdorferi* and host cells. PLoS Pathog. **9:**e1003109. doi:10.1371/journal.ppat.1003109.
8. **Caimano MJ, Eggers CH, Gonzalez CA, Radolf JD.** 2005. Alternate sigma factor RpoS is required for the in vivo-specific repression of *Borrelia burgdorferi* plasmid lp54-borne *ospA* and *lp6.6* genes. J. Bacteriol. **187:**7845–7852.
9. **Caimano MJ, Eggers CH, Hazlett KR, Radolf JD.** 2004. RpoS is not central to the general stress response in *Borrelia burgdorferi* but does control expression of one or more essential virulence determinants. Infect. Immun. **72:**6433–6445.
10. **Caimano MJ, Iyer R, Eggers CH, Gonzalez C, Morton EA, Gilbert MA, Schwartz I, Radolf JD.** 2007. Analysis of the RpoS regulon in *Borrelia burgdorferi* in response to mammalian host signals provides insight into RpoS function during the enzootic cycle. Mol. Microbiol. **65:**1193–1217.
11. **Caimano MJ, Kenedy MR, Kairu T, Desrosiers DC, Harman M, Dunham-Ems S, Akins DR, Pal U, Radolf JD.** 2011. The hybrid histidine kinase Hk1 is part of a two-component system that is essential for survival of *Borrelia burgdorferi* in feeding *Ixodes scapularis* ticks. Infect. Immun. **79:**3117–3130.
12. **Tokarz R, Anderton JM, Katona LI, Benach JL.** 2004. Combined effects of blood and temperature shift on *Borrelia burgdorferi* gene expression as determined by whole genome DNA array. Infect. Immun. **72:**5419–5432.
13. **Ojaimi C, Brooks C, Casjens S, Rosa P, Elias A, Barbour A, Jasinskas A, Benach J, Katona L, Radolf J, Caimano M, Skare J, Swingle K, Akins D, Schwartz I.** 2003. Profiling of temperature-induced changes in *Borrelia burgdorferi* gene expression by using whole genome arrays. Infect. Immun. **71:**1689–1705.
14. **Burtnick MN, Downey JS, Brett PJ, Boylan JA, Frye JG, Hoover TR, Gherardini FC.** 2007. Insights into the complex regulation of *rpoS* in *Borrelia burgdorferi*. Mol. Microbiol. **65:**277–293.
15. **Lybecker MC, Abel CA, Feig AL, Samuels DS.** 2010. Identification and function of the RNA chaperone Hfq in the Lyme disease spirochete *Borrelia burgdorferi*. Mol. Microbiol. **78:**622–635.
16. **Lybecker MC, Samuels DS.** 2007. Temperature-induced regulation of RpoS by a small RNA in *Borrelia burgdorferi*. Mol. Microbiol. **64:**1075–1089.
17. **Sultan SZ, Pitzer JE, Miller MR, Motaleb MA.** 2010. Analysis of a *Borrelia burgdorferi* phosphodiesterase demonstrates a role for cyclic-di-guanosine monophosphate in motility and virulence. Mol. Microbiol. **77:**128–142.

18. **He M, Oman T, Xu H, Blevins J, Norgard MV, Yang XF.** 2008. Abrogation of *ospAB* constitutively activates the Rrp2-RpoN-RpoS pathway (sigma^N-sigma^S cascade) in *Borrelia burgdorferi*. Mol. Microbiol. **70:**1453–1464.
19. **Pappas CJ, Iyer R, Petzke MM, Caimano MJ, Radolf JD, Schwartz I.** 2011. *Borrelia burgdorferi* requires glycerol for maximum fitness during the tick phase of the enzootic cycle. PLoS Pathog. **7:**e1002102. doi:10.1371/journal.ppat.1002102.
20. **Hübner A, Yang X, Nolen DM, Popova TG, Cabello FC, Norgard MV.** 2001. Expression of *Borrelia burgdorferi* OspC and DbpA is controlled by a RpoN-RpoS regulatory pathway. Proc. Natl. Acad. Sci. U. S. A. **98:**12724–12729.
21. **Yang XF, Alani SM, Norgard MV.** 2003. The response regulator Rrp2 is essential for the expression of major membrane lipoproteins in *Borrelia burgdorferi*. Proc. Natl. Acad. Sci. U. S. A. **100:**11001–11006.
22. **Boardman BK, He M, Ouyang Z, Xu H, Pang X, Yang XF.** 2008. Essential role of the response regulator Rrp2 in the infectious cycle of *Borrelia burgdorferi*. Infect. Immun. **76:**3844–3853.
23. **Xu H, Caimano MJ, Lin T, He M, Radolf JD, Norris SJ, Gheradini F, Wolfe AJ, Yang XF.** 2010. Role of acetyl-phosphate in activation of the Rrp2-RpoN-RpoS pathway in *Borrelia burgdorferi*. PLoS Pathog. **6:**e1001104. doi:10.1371/journal.ppat.1001104.
24. **Hyde JA, Shaw DK, Smith Iii R, Trzeciakowski JP, Skare JT.** 2009. The BosR regulatory protein of *Borrelia burgdorferi* interfaces with the RpoS regulatory pathway and modulates both the oxidative stress response and pathogenic properties of the Lyme disease spirochete. Mol. Microbiol. **74:**1344–1355.
25. **Ouyang Z, Deka RK, Norgard MV.** 2011. BosR (BB0647) controls the RpoN-RpoS regulatory pathway and virulence expression in *Borrelia burgdorferi* by a novel DNA-binding mechanism. PLoS Pathog. **7:**e1001272. doi:10.1371/journal.ppat.1001272.
26. **Sze CW, Li C.** 2011. Inactivation of *bb0184*, which encodes carbon storage regulator A, represses the infectivity of *Borrelia burgdorferi*. Infect. Immun. **79:**1270–1279.
27. **Van Laar TA, Lin YH, Miller CL, Karna SL, Chambers JP, Seshu J.** 2012. Effect of levels of acetate on the mevalonate pathway of *Borrelia burgdorferi*. PLoS One **7:**e38171. doi:10.1371/journal.pone.0038171.
28. **Sanjuan E, Esteve-Gassent MD, Maruskova M, Seshu J.** 2009. Overexpression of CsrA (BB0184) alters the morphology and antigen profiles of *Borrelia burgdorferi*. Infect. Immun. **77:**5149–5162.
29. **Karna SL, Sanjuan E, Esteve-Gassent MD, Miller CL, Maruskova M, Seshu J.** 2011. CsrA modulates levels of lipoproteins and key regulators of gene expression critical for pathogenic mechanisms of *Borrelia burgdorferi*. Infect. Immun. **79:**732–744.
30. **Romeo T.** 1998. Global regulation by the small RNA-binding protein CsrA and the non-coding RNA molecule CsrB. Mol. Microbiol. **29:**1321–1330.
31. **Romeo T, Vakulskas CA, Babitzke P.** 2013. Post-transcriptional regulation on a global scale: form and function of Csr/Rsm systems. Environ. Microbiol. **15:**313–324.
32. **Edwards AN, Patterson-Fortin LM, Vakulskas CA, Mercante JW, Potrykus K, Vinella D, Camacho MI, Fields JA, Thompson SA, Georgellis D, Cashel M, Babitzke P, Romeo T.** 2011. Circuitry linking the Csr and stringent response global regulatory systems. Mol. Microbiol. **80:**1561–1580.
33. **Raju BV, Esteve-Gassent MD, Karna SL, Miller CL, Van Laar TA, Seshu J.** 2011. Oligopeptide permease A5 modulates vertebrate host-specific adaptation of *Borrelia burgdorferi*. Infect. Immun. **79:**3407–3420.
34. **Fraser CM, Casjens S, Huang WM, Sutton GG, Clayton R, Lathigra R, White O, Ketchum KA, Dodson R, Hickey EK, Gwinn M, Dougherty B, Tomb JF, Fleischmann RD, Richardson D, Peterson J, Kerlavage AR, Quackenbush J, Salzberg S, Hanson M, van Vugt R, Palmer N, Adams MD, Gocayne J, Weidman J, Utterback T, Watthey L, McDonald L, Artiach P, Bowman C, Garland S, Fuji C, Cotton MD, Horst K, Roberts K, Hatch B, Smith HO, Venter JC.** 1997. Genomic sequence of a Lyme disease spirochaete, *Borrelia burgdorferi*. Nature **390:**580–586.
35. **Mercante J, Edwards AN, Dubey AK, Babitzke P, Romeo T.** 2009. Molecular geometry of CsrA (RsmA) binding to RNA and its implications for regulated expression. J. Mol. Biol. **392:**511–528.
36. **Mercante J, Suzuki K, Cheng X, Babitzke P, Romeo T.** 2006. Comprehensive alanine-scanning mutagenesis of *Escherichia coli* CsrA defines two subdomains of critical functional importance. J. Biol. Chem. **281:**31832–31842.
37. **Ge Y, Old IG, Girons IS, Charon NW.** 1997. The *flgK* motility operon of *Borrelia burgdorferi* is initiated by a sigma 70-like promoter. Microbiology **143**(Pt 5):1681–1690.
38. **Yakhnin H, Pandit P, Petty TJ, Baker CS, Romeo T, Babitzke P.** 2007. CsrA of *Bacillus subtilis* regulates translation initiation of the gene encoding the flagellin protein (*hag*) by blocking ribosome binding. Mol. Microbiol. **64:**1605–1620.
39. **Mukherjee S, Babitzke P, Kearns DB.** 2013. FliW and FliS function independently to control cytoplasmic flagellin levels in *Bacillus subtilis*. J. Bacteriol. **195:**297–306.
40. **Mukherjee S, Yakhnin H, Kysela D, Sokoloski J, Babitzke P, Kearns DB.** 2011. CsrA-FliW interaction governs flagellin homeostasis and a checkpoint on flagellar morphogenesis in *Bacillus subtilis*. Mol. Microbiol. **82:**447–461.
41. **Sze CW, Morado DR, Liu J, Charon NW, Xu H, Li C.** 2011. Carbon storage regulator A (CsrA(Bb)) is a repressor of *Borrelia burgdorferi* flagellin protein FlaB. Mol. Microbiol. **82:**851–864.
42. **Elias AF, Stewart PE, Grimm D, Caimano MJ, Eggers CH, Tilly K, Bono JL, Akins DR, Radolf JD, Schwan TG, Rosa P.** 2002. Clonal polymorphism of *Borrelia burgdorferi* strain B31 MI: implications for mutagenesis in an infectious strain background. Infect. Immun. **70:**2139–2150.
43. **Samuels DS.** 1995. Electrotransformation of the spirochete *Borrelia burgdorferi*. Methods. Mol. Biol. **47:**253–259.
44. **Maruskova M, Esteve-Gassent MD, Sexton VL, Seshu J.** 2008. Role of the BBA64 locus of *Borrelia burgdorferi* in early stages of infectivity in a murine model of Lyme disease. Infect. Immun. **76:**391–402.
45. **Maruskova M, Seshu J.** 2008. Deletion of BBA64, BBA65, and BBA66 loci does not alter the infectivity of *Borrelia burgdorferi* in the murine model of Lyme disease. Infect. Immun. **76:**5274–5284.
46. **Esteve-Gassent MD, Elliott NL, Seshu J.** 2009. *sodA* is essential for virulence of *Borrelia burgdorferi* in the murine model of Lyme disease. Mol. Microbiol. **71:**594–612.
47. **Seshu J, Boylan JA, Hyde JA, Swingle KL, Gherardini FC, Skare JT.** 2004. A conservative amino acid change alters the function of BosR, the redox regulator of *Borrelia burgdorferi*. Mol. Microbiol. **54:**1352–1363.
48. **Seshu J, Esteve-Gassent MD, Labandeira-Rey M, Kim JH, Trzeciakowski JP, Hook M, Skare JT.** 2006. Inactivation of the fibronectin-binding adhesin gene *bbk32* significantly attenuates the infectivity potential of *Borrelia burgdorferi*. Mol. Microbiol. **59:**1591–1601.
49. **Seshu J, Boylan JA, Gherardini FC, Skare JT.** 2004. Dissolved oxygen levels alter gene expression and antigen profiles in *Borrelia burgdorferi*. Infect. Immun. **72:**1580–1586.
50. **Yang X, Goldberg MS, Popova TG, Schoeler GB, Wikel SK, Hagman KE, Norgard MV.** 2000. Interdependence of environmental factors influencing reciprocal patterns of gene expression in virulent *Borrelia burgdorferi*. Mol. Microbiol. **37:**1470–1479.
51. **Labandeira-Rey M, Seshu J, Skare JT.** 2003. The absence of linear plasmid 25 or 28-1 of *Borrelia burgdorferi* dramatically alters the kinetics of experimental infection via distinct mechanisms. Infect. Immun. **71:**4608–4613.
52. **Steere AC, Coburn J, Glickstein L.** 2004. The emergence of Lyme disease. J. Clin. Invest. **113:**1093–1101.
53. **Rosa PA, Tilly K, Stewart PE.** 2005. The burgeoning molecular genetics of the Lyme disease spirochaete. Nat. Rev. Microbiol. **3:**129–143.
54. **Dresser AR, Hardy PO, Chaconas G.** 2009. Investigation of the genes involved in antigenic switching at the *vlsE* locus in *Borrelia burgdorferi*: an essential role for the RuvAB branch migrase. PLoS Pathog. **5:**e1000680. doi:10.1371/journal.ppat.1000680.
55. **Lin T, Gao L, Edmondson DG, Jacobs MB, Philipp MT, Norris SJ.** 2009. Central role of the Holliday junction helicase RuvAB in *vlsE* recombination and infectivity of *Borrelia burgdorferi*. PLoS Pathog. **5:**e1000679. doi:10.1371/journal.ppat.1000679.
56. **Ouyang Z, Deka RK, Norgard MV.** 2011. BosR (BB0647) controls the RpoN-RpoS regulatory pathway and virulence expression in *Borrelia burgdorferi* by a novel DNA-binding mechanism. PLoS Pathog. **7:**e1001272. doi:10.1371/journal.ppat.1001272.
57. **Jutras BL, Bowman A, Brissette CA, Adams CA, Verma A, Chenail AM, Stevenson B.** 2012. EbfC (YbaB) is a new type of bacterial nucleoid-associated protein and a global regulator of gene expression in the Lyme disease spirochete. J. Bacteriol. **194:**3395–3406.
58. **Jutras BL, Verma A, Adams CA, Brissette CA, Burns LH, Whetstine CR, Bowman A, Chenail AM, Zuckert WR, Stevenson B.** 2012. BpaB and EbfC DNA-binding proteins regulate production of the Lyme disease spi-

rochete's infection-associated Erp surface proteins. J. Bacteriol. **194:**778–786.
59. **Wolfe AJ.** 2005. The acetate switch. Microbiol. Mol. Biol. Rev. **69:**12–50.
60. **Kumari S, Beatty CM, Browning DF, Busby SJ, Simel EJ, Hovel-Miner G, Wolfe AJ.** 2000. Regulation of acetyl coenzyme A synthetase in *Escherichia coli*. J. Bacteriol. **182:**4173–4179.
61. **Ristow LC, Miller HE, Padmore LJ, Chettri R, Salzman N, Caimano MJ, Rosa PA, Coburn J.** 2012. The beta(3)-integrin ligand of *Borrelia burgdorferi* is critical for infection of mice but not ticks. Mol. Microbiol. **85:**1105–1118.
62. **Vogel J.** 2009. A rough guide to the non-coding RNA world of Salmonella. Mol. Microbiol. **71:**1–11.